Folding and Unfolding of Polymer Helices in Solution

Alexander I. Norman,*,† Yiwei Fei,†,§ Derek L. Ho,‡ and Sandra C. Greer*,†

Department of Chemical and Biomolecular Engineering and Department of Chemistry and Biochemistry, The University of Maryland College Park, College Park, Maryland 20742, and Polymers Division, National Institute of Standards and Technology, Gaithersburg, Maryland 20899

Received October 2, 2006; Revised Manuscript Received February 1, 2007

ABSTRACT: We have previously shown that poly(ethylene glycol) (PEG) assumes a helical conformation in isobutyric acid. We now show that the formation of helices by PEG in isobutyric acid requires the presence of a trace amount of water: We can make the helices coil and uncoil by adding or removing trace water to/from the solvent. We also show that the similar polymer poly(ethylene imine) (PEI) forms helices in isobutyric acid and that PEG forms helices in isopentanoic and *n*-propanoic acids but not in isobutanol or *n*-butanol. PEI (M_n = 21.8 kg/mol) forms only helices in isobutyric acid, whereas PEG (M_n = 21.0 kg/mol) forms a mixture of helices and coils. Helical PEI (M_n = 21.8 kg/mol) shows a helix-to-coil transition when the temperature is increased to about 50 °C, while PEG (M_n = 21.0 kg/mol) shows a helix-to-coil transition at 40−45 °C. When the trace water in the solution is D_2O, the PEG (M_n = 21.0 kg/mol) helix-to-coil transition moves to a higher temperature of about 56 °C, perhaps due to stronger hydrogen bonding.

Introduction

Poly(ethylene glycol) (PEG) is the world's most important water-soluble polymer,[1−6] and it has many applications in pharmaceutical materials, agricultural applications, and personal care products.[7−9] In the crystal, the PEG[10,11] molecule forms a 7/2 helix: seven monomer units form two helical turns. PEG is soluble in water and in many organic solvents. Hydrogen bonds can form between water molecules and the oxygen atoms of PEG, and thus PEG is very hygroscopic.[12,13]

Poly(ethylene imine) (PEI) differs from PEG in the substitution of −NH− for −O−. PEI also has industrial uses, including as a flocculant in wastewater treatment, as an adhesive modifier, and as a component in ion exchange resins.[14] PEI is also a reagent for the nonviral delivery of DNA and RNA.[15−17] In the crystalline form,[18] the PEI molecules form double-stranded 5/1 helices: 5 monomers in one helical turn. The −NH− group on PEI can both accept and donate hydrogen bonds, and thus PEI is remarkably hygroscopic and exists in air as hydrates.[19,20]

In this paper, we show that both PEI and PEG will form helices when dissolved in carboxylic acids of chain length 3, 4, or 5. We show that the formation of the polymer helices depends on the presence of trace water in the solvents and that the helices will unfold if the trace water is removed and refold when the water is added back. This is in spite of the fact that PEG and PEI form coils, not helices, in pure bulk water.

We have previously studied properties of PEG in isobutyric acid + water, which has an upper critical solution temperature, T_c, at a mass fraction of 39% isobutyric acid.[21,22] We studied the partitioning and fractionation of PEG between the coexisting liquid phases of isobutyric acid and water[23] and the conformations of PEG in isobutyric acid and its aqueous mixtures.[24,25] Our studies showed that (1) the PEG molecules form coils in both H_2O and D_2O, as expected;[24,26] (2) the PEG molecules of molecular mass greater than or equal to 20 kg/mol form helices that coexist with coils in isobutyric acid and its aqueous mixtures;[24] (3) at lower molecular masses (∼2 kg/mol),[24] the PEG molecules form only helices in pure isobutyric acid; (4) at temperatures above about 42 °C in isobutyric acid, the PEG helices unfold to coils;[24] (5) in a solution of isobutyric acid + water at the critical composition, the PEG helices unfold not only at high temperatures but also near the critical temperature;[25] and (6) in HCl, NaOH, or acetic acid, PEG molecules form coils.[24]

Now we examine the effect of replacing the −O− in PEG by an −NH− group (i.e., PEI) and the effect of changing the solvent. We show that PEI molecules in isobutyric acid also fold into helices. We observe helical conformations of PEG in other carboxylic acids: isopentanoic acid and *n*-propanoic acid. We find that PEG does not form helices in alcohols of the same chain length: *n*-butanol or isobutanol.

We want to understand why PEG and PEI molecules form helices in particular solvents. We hypothesized that the helix of either PEG or PEI is stabilized by a hydration layer formed from the small amount of water present in the solution. We tested this hypothesis by altering the hydration layers on the polymers in two ways: (1) by the addition of either urea, which disrupts the hydrogen bonds between the PEG and the water, and (2) by the addition of molecular sieve, which absorbs water. We observed a reduction in helical character in both cases, confirming that the formation of the helices is related to the hydration layer. Moreover, on the readdition of water, the polymers again fold into helices. Still further, if we rehydrate the dried and unfolded polymer with D_2O rather than H_2O, then the temperature of the helix-to-coil transition is increased, indicating that the stronger hydrogen bonds with the D_2O act to stabilize the polymer helices.

Experimental Methods

Materials. The polymer materials were all linear in architecture. Commercial PEG samples (see Table 1) were used without further purification with the exception of 20kOH PEG, which was recrystallized from methanol; both were −OH terminated. PEI (see Table 1) was also used as received; the expected termination is −OH on one end and $-CH_3$ on the other. The polymer materials were not dried before use in the experiments. All molecular masses

* Corresponding authors. E-mail: anorman1@umd.edu; sgreer@umd.edu.
† The University of Maryland College Park.
‡ National Institute of Standards and Technology.
§ Permanent address: Department of Applied Chemistry, Institute of Chemical Engineering, China University of Mining and Technology, Xuzhou, Jiangsu Province, People's Republic of China 221009.

10.1021/ma0622783 CCC: $37.00
Published on Web 03/08/2007

Table 1. PEG and PEI Samples

polymer	lot no.	source	M_w (kg/mol)[a]	M_n (kg/mol)[b]	M_w/M_n[c]
2kOCH_3 PEG	PEG2OCH3-2K	Polymer Source	1.73	1.56	1.11
2kOH PEG	1097453	Fluka	2.20	2.10	1.05
20kOH PEG	425182/1	Fluka	23.8	21.0	1.14
25k PEI	H08Q19	Alfa Aesar	30.4	21.8	1.39

[a] Weight-average molecular mass. [b] Number-average molecular mass. [c] Polydispersity index.

were determined by size exclusion chromatography in our laboratory, as described below and shown in Table 1.

The solvents used were isobutyric acid (IBA, Aldrich, 99% purity), deuterated isobutyric acid (d-IBA, Isotech, 98% D), D_2O (Aldrich, 99.9% D), isovaleric acid (isopentanoic acid, Sigma Aldrich, 98% purity), isobutanol (J.T. Baker, 99.8% purity), *n*-butanol (Fisher Scientific, 99.9% purity), and *n*-propanoic acid (Markovnikov Chemicals). H_2O was obtained from a purification system (Barnstead, 18.2 MΩ cm). The chiral dopants used in all the polarimetry experiments were (*S*)-(+)-1,2-propanediol or (*R*)-(−)-1,2-propanediol (Lancaster Chemicals, 98% pure enantiomer), (*S*)-(+)-2-butanol (Aldrich, 99% pure enantiomer), and (*R*)-(+)-styrene oxide (Sigma-Aldrich, 97% pure enantiomer).

Urea pellets (J.T. Baker, 99.3% purity) were ground into a fine powder. Davison type 4A sodium aluminosilicate molecular sieve (4 Å pore size) was washed several times with deionized water and dried in a vacuum immediately prior to use.

The polymer concentrations in the solutions studied were 12 ± 1 mg/mL, consistent with our previous work.[24]

Size Exclusion Chromatography (SEC). The Waters SEC system has been described previously.[24] For the PEG samples, a mobile phase of pure H_2O (see above) was used. For the PEI samples, a buffer solution of 0.5 M sodium acetate + 0.5 M acetic acid (pH = 7.0) was used. The apparatus was calibrated with PEG standards (American Standards Corp., Mentor, OH). Each sample was diluted to ≤2 mg/mL in pure H_2O, and then a volume of 100 μL was injected for a run time of 60 min at a flow rate of 0.6 mL/min. The chromatograms were analyzed using the Waters software package Breeze (version 3.30). All measurements were carried out at 30 °C.

Small-Angle Neutron Scattering (SANS). SANS measurements on PEG have been reported previously.[24] For the new SANS measurements on PEI, 25k PEI was dissolved in both D_2O and deuterated isobutyric acid. SANS from each PEI sample was measured at temperatures of 30, 45, and 60 °C. SANS measurements were carried out on beamline NG3 (30 m SANS) at the National Institute of Standards and Technology Center for Neutron Research (NCNR) in Gaithersburg, MD,[24,27] and reduced as described previously.[24]

We analyze the SANS data in four ways: (1) analyzing the slope of $I(q)$, (2) modeling of the data to specific models available from NCNR that describe particle shape and interaction, (3) taking the Fourier transformation of the data into real space using the generalized indirect Fourier transform (GIFT) method,[28] and (4) using a second Fourier transform procedure, low-resolution shape (LORES).[29]

In the analysis of the slope of $I(q)$ over a given q range,[30] the Guinier regime at low q gives information about the radius of gyration, R_g, of the polymer. Over intermediate q ranges (0.03−0.15 $Å^{-1}$) information relating to the particle shape is obtained: The slope is −1 for a rigid rod, −2 for a random coil, and −1.67 for a flexible chain with excluded volume.[30] The data at high q values ($q > 0.28$ $Å^{-1}$) are in the Porod regime, where a slope in $I(q)$ of about −4 indicates a sharp interface between particle and solvent.[31]

The second method of SANS analysis is modeling with methods developed at the NCNR.[32] For PEI in deuterated isobutyric acid, we use the cylinder model.[33] The model estimates the cross-sectional radius and length of the polymer cylinder, with the volume fraction of polymer and the scattering length densities of the solvents kept fixed. The model assumes circular cross sections and a monodisperse chain length. For PEI in D_2O, we use a model of a semiflexible chain with excluded volume.[34] The Kuhn length, b, is determined by the semiflexible chain model and characterizes the stiffness of the polymer chain.

The third method of SANS data analysis is the Fourier transformation of the scattered intensity, $I(q)$, into the real space pair distance distribution function, $p(r)$, where r is the distance. The $p(r)$ is a histogram of the distances between pairs of different volume elements within the same scattering object. We obtain $p(r)$ from the SANS data using the generalized indirect Fourier transformation (GIFT) method of Glatter and co-workers.[28,35] The method is available as part of the PCG software (version 1.01.02).[36] The GIFT method is able to account for interparticle interactions, but in the cases here the polymer concentrations are low enough that such interactions can be ignored. Hence, this method of analysis is model-independent. The $p(r)$ provides additional information regarding the shape, dimension, and flexibility of the scattering object.[35,37−39] Spherical particles give rise to a perfectly symmetric $p(r)$ about a central maximum. Rodlike particles will display a very sharp peak in $p(r)$ at low values of r, with a point of inflection that corresponds to the cross-sectional diameter, and then a decrease at higher r (linearly if perfectly rigid, undulating somewhat if not rigid) to a point where $p(r) = 0$. This point $p(r) = 0$ determines the length of the rod, or the maximum particle dimension, D_{max}.

The final method of data analysis that we use is low-resolution shape (LORES).[29] This program (available from greguric@umbc.edu) determines the three-dimensional low-resolution shape of macromolecules based on the optimization of a SANS profile to experimental data. Unlike GIFT, this method is dependent on a model: sphere, cylinder, right/left handed helix, etc. The LORES program generates a three-dimensional model based on a number of input parameters and an initial geometric shape, which is then transformed into a scattering intensity profile. The experimental data are compared to this model, and the model dimensions are changed until the comparison between model and data satisfies the program tolerance. The outputs of this program are the normalized $p(r)$ profile, the normalized scattering profile, $I(q)$ vs q, and the optimized geometric parameters and coordinates (PDB format) for a low-resolution three-dimensional model.

In summary, the scaling analysis of $I(q)$ gives the general shape of the scattering molecule, the model analysis gives the dimensions of model geometries fitted to the data, the GIFT analysis gives a two-dimensional model-free analysis of the three-dimensional scatterer, and the LORES analysis gives a model-dependent three-dimensional analysis of the data. The first three methods can distinguish between a rod and a coil, but not between a rod and a helix. The third method can fit an assumed model helix to the data.

Polarimetry. In earlier work, we developed a technique for detecting polymer helices by polarimetry for polymers that normally form enantiomeric mixtures of helices, half left-handed and half right-handed,[24,25] and thus show no optical rotation. We use the addition of a chiral dopant to the polymer mixture at high temperatures, where the polymers are in the coil configurations.[40] Then when the solution is cooled, the dopant causes a bias in the folding of the polymers into helices, resulting in an enantiomeric excess. We use the resulting optical rotation due to the polymer to monitor the presence and the folding and unfolding of the polymer helices.

It is likely that not only is the polymer affected by the dopant, but that also the dopant is affected by the polymer, and thus that the "background" optical rotation of the dopant itself changes upon the addition of the polymer. A study of this issue is given in the Supporting Information, where we show that we obtain basically the same polarimetry profile for PEG in isobutyric acid when using

two different dopants. That two different dopants give the same results supports our use of polarimetry on doped samples to monitor the presence or absence of helical polymers.

For all the polarimetry measurements, a sample of PEG or PEI was dissolved in the solvent to a concentration of 12 ± 1 mg/mL. The chiral dopant was added to the polymer solution to a mass fraction of 2×10^{-3}. All samples were preheated on a stirrer hot plate to about 80 °C, vigorously stirred, and then allowed to cool to room temperature prior to measurements.

The Jasco P1010 polarimeter and its temperature control/measurement system have been described previously.[24] The temperature was controlled to an accuracy and precision of about 0.1 °C.

For all the polarimetry measurements, the background signal was measured on the empty cell and then on the solvent alone, with no polymer and no dopant. Then the optical rotation was measured of the solvent + chiral dopant as a function of temperature, on heating and on cooling, twice. The polymer was added to the solvent + dopant mixture, and the optical rotation was measured again on heating and cooling. For each data point, the sample was allowed to reach equilibrium (~15 min) before the next measurement was taken. The optical rotation of the solvent + dopant mixture at each temperature was subtracted from the optical rotation of the solvent + dopant + polymer mixture at that temperature to obtain a net optical rotation. The net optical rotation, α, was converted to a specific optical rotation, $[\alpha] = \alpha/lc$, where l is the path length in dm and c is the polymer concentration in mg/mL.

Perturbation of Water of Hydration. The polymer samples in our experiments were used without further purification and without drying. Since both PEG and PEI are hygroscopic, we would expect that each would include adsorbed water. We hypothesized that a water of hydration could have a role in the formation of the helices.

We perturbed the water of hydration in three different ways: (i) the addition of urea, (ii) the addition of molecular sieve, and (iii) the addition of D_2O to polymer solution that had been dried by molecular sieve. Urea reduces hydrogen bonding.[41] Molecular sieves remove water from the solution. Hydrogen bonding is stronger in D_2O than in H_2O,[42] so we would expect rehydration by D_2O to make a stronger hydration layer and thereby increase the temperature of the helix-to-coil transition.

The optical rotation of the polymer solution was measured at room temperature after the addition of the urea or molecular sieve and equilibration for few hours. The sample was then rehydrated with one drop of H_2O or D_2O and shaken, and measurements of optical rotation were taken over a few hours. The temperature of the helix-to-coil transition was also determined following D_2O or H_2O addition.

Results and Discussion

The uncertainties and error bars on all SANS graphs and calculations are given as one standard deviation. The uncertainties and error bars on all polarimetry graphs are given as three standard deviations.

1. Small-Angle Neutron Scattering (SANS). New measurements were made on 25k PEI in deuterated isobutyric acid and in D_2O. We compare these data to SANS data previously reported on the same 20kOH PEG sample listed in Table 1.[24] Note that the polymer samples are polydisperse (Table 1), and thus the parameters obtained from SANS data analysis are averages over the molecular mass distributions.

1.1. Solvent = D_2O. The SANS data for both polymers in D_2O indicate that the polymers assume coil conformations in D_2O, at temperatures from 30 to 60 °C. Figure 1 shows plots of $I(q)$ for 20kOH PEG[24] and for 25k PEI, both in D_2O at 60 °C. Note that there is more scatter in the data for PEI than in the data for PEG; this scatter was even worse at lower temperatures, so we analyze only the 60 °C data here.

Guinier analysis of the data at low q in Figure 1 gives radii of gyration of the polymer coils, R_g, of 46.0 ± 0.6 Å for PEG and 78 ± 4 Å for PEI. This result is very dependent on the q range of the analysis, particularly when there is an increase in $I(q)$ at low q due to aggregation, as seen in Figure 1 for PEI. The slope of $I(q)$ at intermediate q is −1.57 ± 0.02 for 20kOH PEG and −1.8 ± 0.2 for 25k PEI, both consistent with the scaling of semiflexible chains, for which $I(q)$ has a slope of −5/3.[34] If the scattering were from rigid rods, $I(q)$ would scale as −1, and if it were from random coils, $I(q)$ would scale as −2.[30] The scaling at high q is −2.7 ± 0.3 for 20kOH PEG and −2.3 ± 0.3 for 25k PEI, both inconsistent with scattering from sharp interfaces, such as rigid rods, where $I(q)$ scales as −4, again supporting the conclusion that both polymers are coils in D_2O.

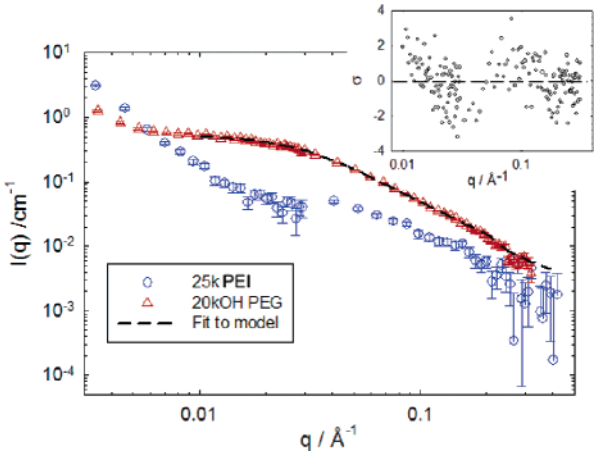

Figure 1. SANS intensity, $I(q)$, for 25k PEI and 20kOH PEG[24] in D_2O at 60 °C. For clarity, only every third data point has been plotted, and the data for 20kOH PEG have been shifted along the y-axis by a factor of 10. The broken line indicates the fit of a semiflexible chain model for the PEG; the residual plot to this fit is shown in the inset.

Next the NCNR models were applied to the data in Figure 1. The 20kOH PEG in D_2O was successfully modeled as semiflexible chains with excluded volume;[24,34] the parameters from the fit are given in Table 2. For 25k PEI, the modeling proved unsuccessful: The errors associated with the fitted parameters were more than the values of the parameters themselves.

Then the GIFT procedure was applied to the SANS data for the polymers in D_2O. Figure 2 shows the resulting $p(r)$ for 20kOH PEG and for 25k PEI in D_2O at 60 °C. In both cases, $p(r)$ is like that of a skewed sphere. Table 2 lists the parameters obtained from the GIFT analysis, which are consistent with the Guinier analysis. We did not perform a LORES analysis on these data.

In summary, in D_2O both PEG and PEI molecules form coils. The R_g from the Guinier analysis and the $p(r)$ from the GIFT analysis indicate much larger coils for PEI than for PEG. The molecular mass of the PEI is only 4% larger than that of the PEG, so that difference does not account for the difference in coil size. From the $p(r)$, both polymer chains fold into distorted spherical coils in D_2O, but the PEI coils are more spherical than the PEG coils. PEI can both donate and accept hydrogen bonds and thus may be better solvated in D_2O than PEI; perhaps this solvation is the reason for the difference in coil size and shape.

1.2. Solvent = Deuterated Isobutyric Acid (d-IBA). Figure 3 shows $I(q)$ for 20kOH PEG[24] and 25k PEI in deuterated isobutyric acid at 30 °C. The noise in the PEI data at low q precluded a Guinier analysis. $I(q)$ at intermediate q has slopes of −1.08 ± 0.02 for 20kOH PEG and −0.91 ± 0.05 for 25k PEI, both indicating the scatterers to be rigid rods. The slopes at high q are consistent with the scattering from the sharp

Table 2. Parameters from Analysis of SANS Data[a–c]

polymer	solvent	T (°C)	helix or coil?	parameters from modeling (Å)	parameters from GIFT (Å)
2kOCH$_3$ PEG	d-IBA + D$_2$O ($\Phi_{d-IBA} = 0.39$)	60	helix	cylinder:	$R = 5.0 \pm 0.9$,
				$L_1 = 39.6 \pm 0.5$, $R = 4.9 \pm 1.6$, $\chi^2 = 2.03$ (NCNR)	$D_{max} = 45.0 \pm 0.9$
				$L_1 = 43$, $R = 5$ (LORES)	
				helix:	
				$L_1 = 44$, $R = 5$, 11.6 helical turns of length = 3.8 (LORES)	
20kOH PEG	D$_2$O	60	coil	semiflexible chain (NCNR):	$R_g = 41.3 \pm 1.2$ (46.0 ± 0.6), $D_{max} = 150 \pm 1$
				$L_2 = 618 \pm 9$, $b = 15 \pm 0.3$, $R = 2.9 \pm 0.2$; $\chi^2 = 1.65$	
	d-IBA	30	helix + coil	N/A	$R = 5.0 \pm 0.9$, $R_g = 38.5 \pm 0.9$ (42.4 ± 0.6), $D_{max} \sim 150$
		60	coil	N/A	$R_g = 40.0 \pm 0.6$ (46.0 ± 0.6), $D_{max} = 190 \pm 1.2$
25k PEI	D$_2$O	60	coil	N/A	$R_g = 72.5 \pm 0.9$ (78 ± 4), $D_{max} = 194 \pm 0.9$
	d-IBA	30	helix	cylinder (NCNR): $R = 5 \pm 2$, $L_1 = 39 \pm 1$; $\chi^2 = 1.64$	$R = 5.0 \pm 0.7$, $D_{max} = 50.0 \pm 0.7$
		60	helix	cylinder (NCNR): $R = 6 \pm 2$, $L_1 = 25 \pm 1$; $\chi^2 = 1.66$	$R = 5.2 \pm 0.5$, $D_{max} = 34.7 \pm 0.7$

[a] d-IBA is deuterated isobutyric acid, L_1 is the cylinder or helix length, L_2 is the contour length, b is the Kuhn length, R is the radius of the chain or the helical radius, R_g is the radius of gyration, D_{max} is the maximum dimension, χ^2 indicates the goodness of fit, and T is the temperature. [b] Parameters were obtained from both modeling and from the $p(r)$ function. Values of R_g in parentheses are those determined from Guinier plots. D_{max} is the maximum particle dimension, and for pure helices this is equivalent to L. [c] Errors are given as one standard deviation.

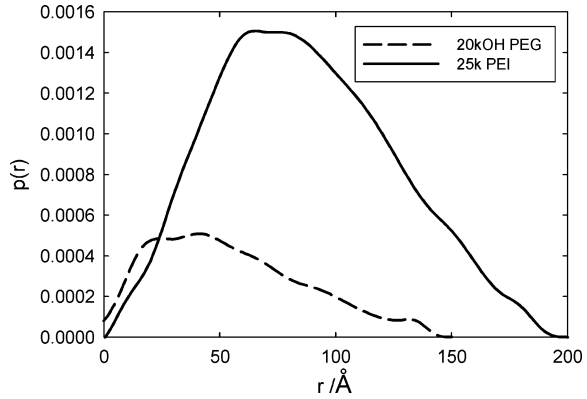

Figure 2. The pair distance distribution function, $p(r)$, for 20kOH PEG and 25k PEI in D$_2$O at 60 °C. The difference in intensity of $p(r)$ between the two is just due to a difference in data acquisition time.

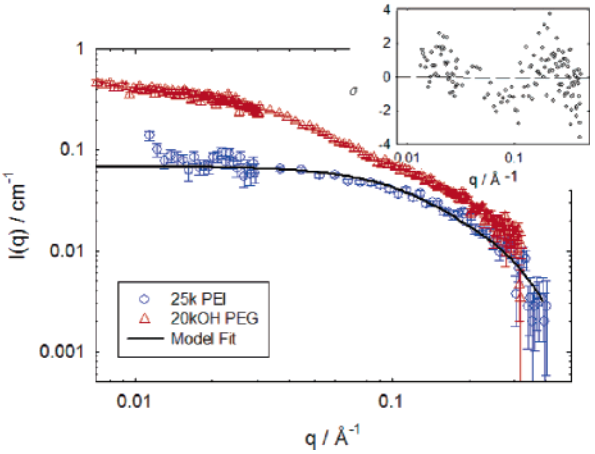

Figure 3. SANS intensity, $I(q)$, for 25k PEI and 20kOH PEG in deuterated isobutyric acid at 30 °C. For clarity, only every third data point has been plotted. The solid line shows the fit of a cylinder model to the 25k PEI data; the inset shows the residual plot for this fit.

interfaces of rods: −4.0 ± 0.1 for 20kOH PEG and −4.4 ± 0.9 for 25k PEI.

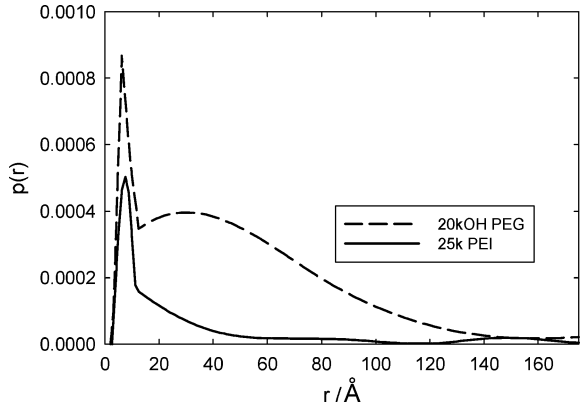

Figure 4. The pair distance distribution functions, $p(r)$, for 20kOH PEG[24] and 25k PEI in deuterated isobutyric acid at 30 °C, as obtained from the GIFT analysis.

The solid line in Figure 3 shows the NCNR cylinder model as successfully fitted to the data for 25k PEI (see dimensions in Table 2). We do not show a cylinder model fit for 20kOH PEG because (see GIFT analysis below[24]) this polymer forms both rods and coils in deuterated isobutyric acid, which makes modeling problematic.

The GIFT analysis gives $p(r)$ for 20kOH PEG and 25k PEI in deuterated isobutyric acid at 30 °C (Figure 4). The $p(r)$ for 25k PEI has the form indicating that the scatterers are entirely rods. The linear region of $p(r)$ for PEI indicates that the rod is rigid: Should any axial inhomogeneity be present, this would result in undulations in $p(r)$ in this region; for example, wormlike micelles[43] show such undulations in $p(r)$. Dimensions from the GIFT analysis for PEI are given in Table 2: The radii are consistent between the cylinder modeling and the GIFT analysis. D_{max} from the GIFT analysis and the cylinder length L_1 from the cylinder modeling differ significantly, and D_{max} differs between the 30 °C and 60 °C data; we attribute this lack of consistency to the scatter in $I(q)$ at low q for the PEI data in isobutyric acid.

The $p(r)$ for 20kOH PEG in deuterated isobutyric acid in Figure 4 shows a coexistence of rods and coils.[24] The sharp

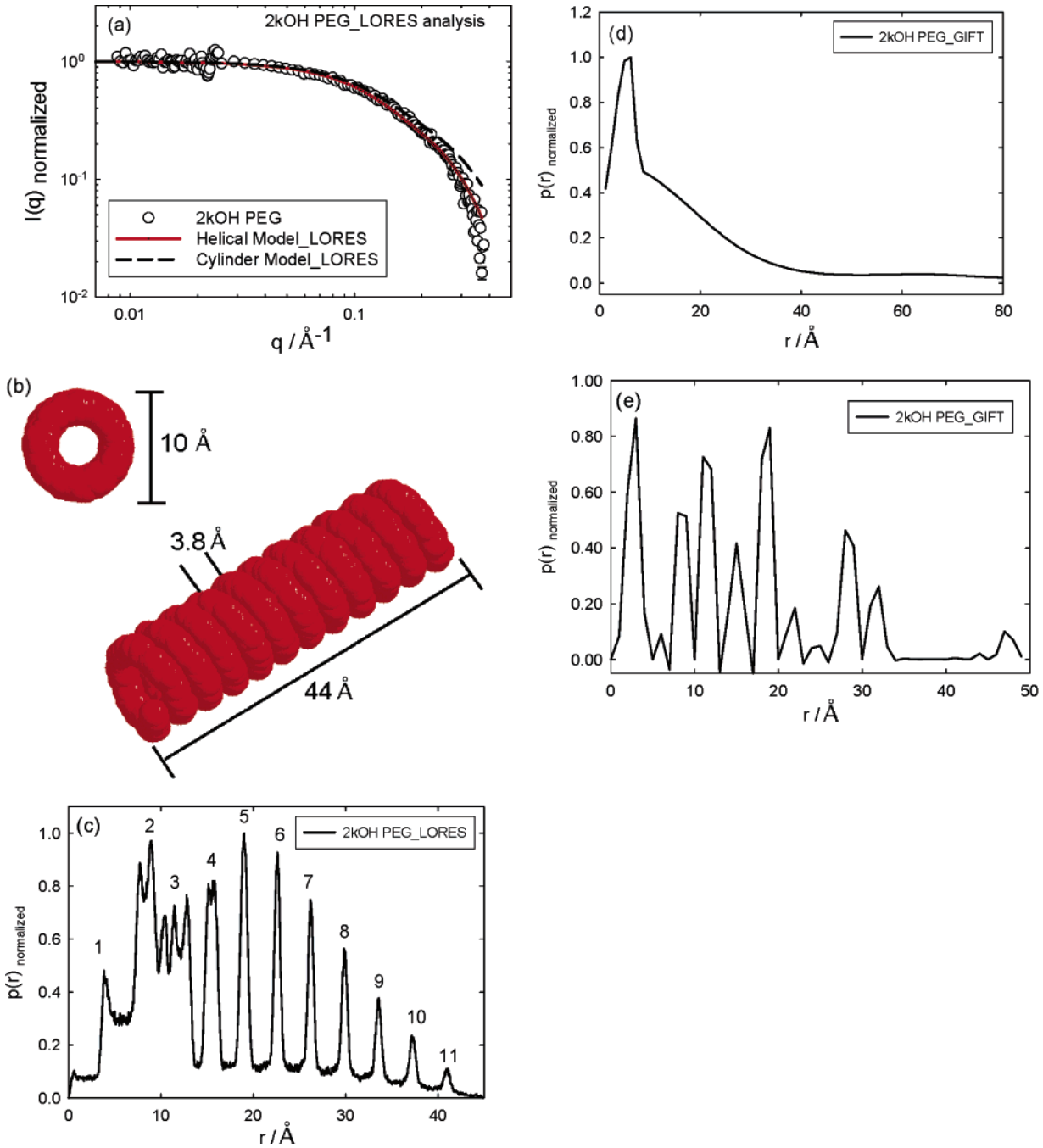

Figure 5. (a) SANS profile $I(q)$ for $2kOCH_3$ PEG in deuterated isobutyric acid at 60 °C; the broken black line shows the LORES fit for a cylinder, and the solid red line shows the LORES fit for a right-handed helical model. (b) The three-dimensional model of the right-handed helix obtained from the LORES analysis. (c) *p(r)* obtained from a LORES analysis with a right-handed helical model, where the numbers above each peak represent the number of each helical turn. (d) *p(r)* obtained from GIFT analysis with unevenly distributed spline functions. (e) Evenly distributed spline functions.

peak at lower r indicates rods, while the broader peak at higher r indicates coils;[44] dimensions are given in Table 2. The determination of D_{max}, the maximum particle size, is difficult when both coils and rods are present, but we estimate it to be about 150 Å. It is not possible to get a reliable dimension for L_1 in this case.

Our previous study[24] showed that the smaller molecular mass $2kOCH_3$ PEG in deuterated isobutyric acid formed only rods, with no coexistence of coils, with $L_1 = 40.0 \pm 1.2$ Å, which is similar to L_1 for 25k PEI (40−50 Å). Thus, the longer PEI molecule forms a rod of about the same length as the shorter PEG molecule, implying that PEI forms tighter helices than PEG when dissolved in deuterated isobutyric acid. Indeed, in the crystals, the PEI helix (5/1) is more tightly wound than the PEG helix (7/2). These differences may be related to the fact that PEI is more hygroscopic than PEG and to our hypothesis that the water of hydration effects and affects the formation of the polymer helices (see below).

LORES analysis was not successful for the SANS data for PEI in isobutyric acid because of the high level of noise in the data. However, we successfully used LORES and GIFT to reanalyze the SANS data reported previously for $2kOCH_3$ PEG in deuterated isobutyric acid, where only rodlike conformations exist.[24] These SANS data and fits to them by cylindrical and helical LORES models are shown in Figure 5a and Table 2. The helical LORES model assumes a 7/2 helix. The experi-

mental data are fitted better by the helical model, deviating from the cylindrical model at about 0.25 $Å^{-1}$. The LORES fit parameters are consistent with those from the GIFT analysis and with those from a NCNR core−shell cylinder model.[24] The helical LORES model predicts the number of helical turns of this PEG chain of $M_n = 1.73$ kg/mol to be 11.6. Studies of the PEG helix by X-ray crystallography and by scanning tunneling microscopy[10,11] have shown the PEG helix in the solid state to have an average outer diameter of 7.6 Å, consistent with the maximum outer diameter of 10 Å in Figure 5b, but a length of 2.9 Å per monomer, larger than the 1.1 Å per monomer for the structure in Figure 5b. It is not unreasonable for the helix in a poor solvent to be more tightly wound than in the crystal.

The $p(r)$ profile generated by LORES for a helical PEG conformation is shown in Figure 5c and shows a number of peaks, the position of each peak corresponding to the length of a helical turn. The data become noisy at low values of r due to the larger errors associated with SANS data at high q values. There are 11 main peaks that are equidistant in r (numbered in Figure 5c), relatively consistent with the number of helical turns in the polymer helix (11.6). The mean length of a helical turn is 3.7 ± 0.1 Å, consistent with Figure 5b.

We can compare the helical $p(r)$ for $2kOCH_3$ PEG obtained from the LORES analysis (Figure 5c) to the helical $p(r)$ obtained from the GIFT analysis (Figure 5d,e) for this same sample. While the GIFT analysis is model-independent, the choice of how the spline functions are distributed in q can affect the $p(r)$ profile. The analysis for the rod structures of $2kOCH_3$ PEG (Figure 5d) used more spline functions at lower q in order to extract the rod dimensions with more resolution, but used a lower resolution at higher q. If instead we distribute the spline functions evenly in q, we obtain the $p(r)$ topology shown in Figure 5e. This form of $p(r)$ is closer to what is expected for a helix, where the peaks appear to represent the turns of the helix. This analysis is consistent with that from LORES: There are 13 main peaks which are approximately equidistant in r, relatively consistent with the number of helical turns in the polymer helix (11.6 from LORES), and the mean length of a helical turn using the GIFT method is 3.8 ± 0.8 Å (same as for LORES).

In summary, the SANS data indicate coil conformations in D_2O for both PEG and PEI, rod conformations of PEI and low molecular mass PEG in isobutyric acid, and mixtures of rod and coil conformations of higher molecular mass PEG in isobutyric acid. If we assume that the rods are, in fact, helices, then we can fit helical models to the SANS data for PEG and derive dimensions of the polymer helices. The dimensions of the PEI rods indicate that the PEI helices are more tightly wound than the PEG helices.

2. Polarimetry. Note that the polarimetry studies were all done in hydrogenated solvents, not in the deuterated solvents used for the SANS studies. From our previous study[24] on 20kOH PEG we know that PEG exhibits no optical rotation in H_2O containing a chiral dopant, and that PEG exhibits no optical rotation in isobutyric acid without a chiral dopant, but that PEG does exhibit a net optical rotation in isobutyric acid with a chiral dopant—evidence that the PEG rods seen by SANS are indeed helices and that the optical rotation of PEG in doped isobutyric acid vanishes at higher temperature due to a helix-to-coil transition.

A polarimetry run for PEI in H_2O + chiral dopant showed no net optical rotation, indicating the absence of helical conformations of PEI in H_2O. New measurements were made on 20kOH PEG and 25k PEI solutions in isobutyric acid, propanoic acid, isopentanoic acid, *n*-butanol, and isobutanol, at several temperatures. In addition, measurements were made on 2kOH PEG in isobutyric acid at several temperatures. The measurements above were all made with the dopant (*S*)-1,2-propanediol, and then two other chiral dopants were used for 20kOH PEG in isobutyric acid: (*R*)-(+)-styrene oxide and (*S*)-(+)-2-butanol. Graphs of the polarimetry data are available online in the Supporting Information. Temperatures of the helix-to-coil transitions are summarized in Table 3.

Table 3. Observed Helix-to-Coil Transition Temperatures (in °C)

polymer	T_t(d-IBA)[a]	T_t(h-IBA)[b]	T_t(h-PPA)[c]	T_t(h-IPA)[d]
2kOH PEG	?>60[e]	?>70	N/A	N/A
20kOH PEG	55−60	42	?>80	?>70
25k PEI	?>60	50	N/A	N/A

[a] Deuterated isobutyric acid. [b] Isobutyric acid. [c] Propanoic acid. [d] Isopentanoic acid. [e] The notation "?>" indicates that no transition was observed below the given temperature.

2.1. Effect of Changing the Polymer. 25k PEI in isobutyric acid does show a net optical rotation, indicating the presence of polymer helices. The optical rotation decreases as the temperature increases, indicating the unfolding of the helices into coils. The data become more reproducible on thermal cycling, and if we take the later cycles as the more reliable data, the helix-to-coil transition is observed at about 42 °C for 20kOH PEG and at about 50 °C for 25k PEI (Table 3). We previously reported a helix-to-coil transition temperature of 68 °C for 20kOH PEG in isobutyric acid;[24] we now believe that this was incorrect because the error bars were underestimated. In the SANS experiments (see above, section 1.2) in *deuterated* isobutyric acid, the 20kOH PEG showed a helix-to-coil transition between 55 and 60 °C, but the 25k PEI still remained in helical form at 60 °C.

Thus, PEI does have helical conformations in isobutyric acid, and those helices are stable to higher temperatures than are PEG helices. Also, the polymer helix-to-coil transitions occur at higher temperatures in deuterated isobutyric acid than in "hydrogenated" isobutyric acid, which is to be expected if the helices are stabilized by hydrogen bonds, given that D-bonds are stronger than H-bonds.

2.2. Effect of Changing the Solvent. First we tested the effect of changing the carbon chain length in the carboxylic acid solvent by measuring the optical rotation of 20kOH PEG in propanoic acid, one carbon *shorter* in chain length than isobutyric acid. Polarimetry indicates that propanoic acid leads to a more stable polymer helix: no helix-to-coil transition occurs even up to 80 °C. For 20kOH PEG in isopentanoic acid, one carbon atom *longer* in chain length than isobutyric acid, the effect is the same: there is no helix-to-coil transition in this temperature range.

Then we tested the effect of a change of the functional group of the solvent: Is the $-CO_2H$ group required for these polymers to form helices? Polarimetry measurements for 20kOH PEG in both *n*-butanol and isobutanol showed no net optical rotation, indicating that 20kOH PEG molecules do not form helices in either *n*-butanol or isobutanol.

We conclude that the ability of the polymer to form a helix is not governed by the conformation of the carbon backbone of the solvent, since isobutanol and isobutyric acid have the same carbon framework, but seems to be related to the functional group, since carboxylic acids lead to helices and their alcohols do not. On the other hand, our prior study[24] showed that PEG does not form helices in acetic acid, so the formation of polymer helices requires at least three carbons in the carboxylic acid.

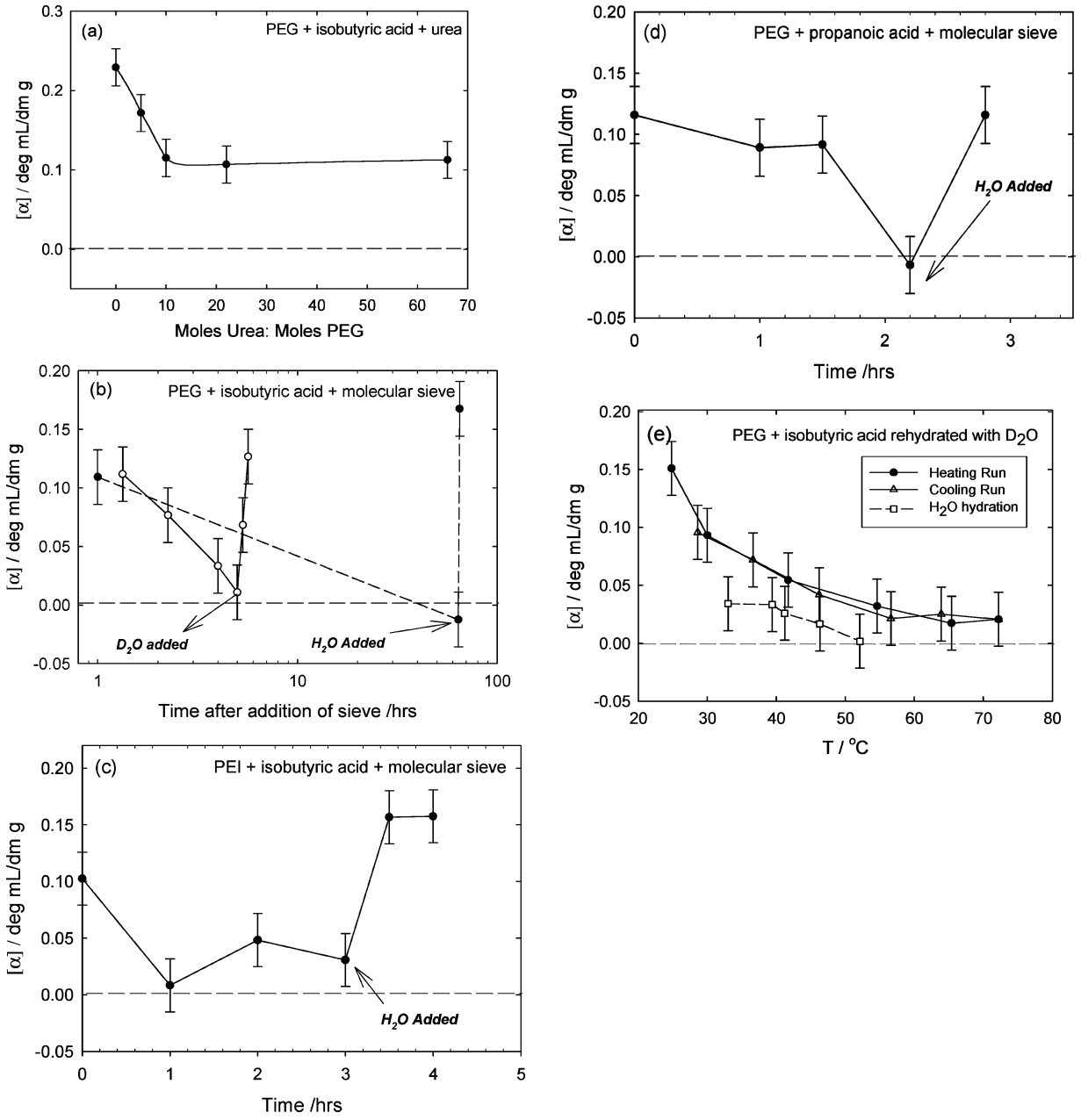

Figure 6. Specific optical rotation of (a) 20kOH PEG in isobutyric acid doped with (*S*)-1,2-propanediol, as a function of urea concentration; (b) 20kOH PEG in isobutyric acid doped with (*S*)-1,2-propanediol after the addition of molecular sieve, as a function of time, for two different sample runs (open and closed circles); (c) 25k PEI in isobutyric acid doped with (*S*)-1,2-propanediol after the addition of molecular sieve, as a function of time; and (d) 20kOH PEG in propanoic acid doped with (*S*)-1,2-propanediol after the addition of molecular sieve, as a function of time. (e) Specific optical rotation of 20kOH PEG in isobutyric acid doped with (*S*)-1,2-propanediol, rehydrated with D_2O. In (b)−(d), where molecular sieve was used to remove water, water was later added to rehydrate the polymers, at the times indicated. All error bars represent three standard deviations.

2.3. Effect of Changing the Polymer Molecular Mass. When the molecular mass of PEG is changed from M_w = 23.8 kg/mol (20kOH PEG) to 2.20 kg/mol (2kOH PEG), polarimetry indicates that helices still form in isobutyric acid. As the temperature is increased from 20 to 75 °C, the optical rotation signal decreases somewhat but does not go to zero, so the helices are still stable at the higher temperatures (see Supporting Information, Figure S4). These measurements agree with our previous SANS results which showed that $2kOCH_3$ PEG remains a rigid rod at 60 °C, whereas 20kOH PEG reverts to a coil at that temperature.[24]

We conclude that PEG of lower molecular mass forms helices that are stable to higher temperatures than are the helices formed by PEG of higher molecular mass. It is reasonable that helices in small polymers are more stable than those in larger polymers, since it is more likely for the long polymer to have "errors" in folding or even to have unfolded regions.

2.4. Perturbation of Water of Hydration. We postulated that the polymer helices are stabilized by a hydration shell of water molecules that is formed by hydrogen bonding between the −O− or −NH− of the polymer backbone and the trace water in the organic solvent. To test this hypothesis, we perturbed the hydration water by adding urea or by adding a molecular sieve. We then tested the reversibility of the effect by adding H_2O or D_2O to the solvent that had been dried by molecular sieve. These studies were at a constant 25 °C.

Figure 6a shows the observed optical rotation as urea is added to 20kOH PEG in isobutyric acid doped with (*S*)-1,2-propanediol: [α] decreases as the concentration of urea increases. Urea disrupts hydrogen bonding,[41] and the decrease in signal

can be taken to indicate an uncoiling of the polymer helices due to loss of hydrogen bonds. However, the optical rotation reaches a plateau at a molar ratio of urea to PEG of about 22 and does not go to zero as more urea is added. At the higher urea concentrations, the urea was hard to dissolve and heating with vigorous stirring was necessary. Thus, the plateau in the optical rotation is probably because no more urea will dissolve in the solvent. The urea did disrupt the hydrogen bonding and reduce the polymer helicity, but the helicity was not completely destroyed.

Figure 6b−d shows the effect of the addition of molecular sieve on the optical rotation of PEG or PEI. Figure 6b shows the experiment for 20kOH PEG in isobutyric acid: When the sieve was allowed equilibrate in the sample that was stirred for 60 h (filled symbols), the optical rotation completely disappeared. Upon the addition of one drop of H_2O to the sample, the optical rotation signal returned to its initial value within 1 h. These measurements were repeated weeks later and are shown in Figure 6b as open symbols. The data reproduce well and show that the signal disappears after about 5 h exposure to the molecular sieve. On rehydration with D_2O, the signal comes back. Figure 6c,d shows the effect of molecular sieve for 25k PEI in isobutyric acid and for 20kOH PEG in propanoic acid. The signal disappears more quickly for 25k PEI in isobutyric acid than for 20kOH PEG in isobutyric acid; on rehydration, the signal returns, but takes longer to return.

The main observation is the same in all experiments: The addition of molecular sieve dehydrates the system, which causes the observed optical rotation to disappear: The polymer helices revert to coils. On rehydration of the system, the observed optical rotation returns to nearly its initial value: The polymer coils fold back into helices. Thus, the trace water plays a crucial role in the formation and stability of these polymer helices in nonaqueous solvents.

Our final experiment was to observe what happened when the dehydrated polymer solutions were rehydrated with D_2O instead of with H_2O. We hypothesized that, since D_2O forms stronger hydrogen bonds than H_2O,[42] the stability of the helices will be greater, and thus the helix-to-coil transition will occur at a higher temperature, if the polymer hydration shell consists of D_2O instead of H_2O. The optical rotation indicated that the sample did rehydrate with D_2O and re-form the polymer helices (Figure 6b). Figure 6e shows the optical rotation as a function of temperature for the sample rehydrated by D_2O: There is a significant change in the temperature of the helix-to-coil transition temperature, T_t, when the sample is rehydrated with D_2O: T_t is about 42 °C in the presence of trace H_2O prior to the addition of molecular sieve, and T_t is about 56 °C after the addition of molecular sieve and subsequent rehydration with D_2O. Polarimetry studies were not conducted in deuterated isobutyric acid because this solvent is very expensive. The increased helix-to-coil transition temperature when the rehydrating agent is D_2O is more evidence for the crucial role of trace water in the formation and stability of PEG helices in certain nonaqueous solvents.

Conclusions

Small-angle neutron scattering data (analyzed by four different methods), combined with polarimetry measurements in the presence of chiral dopants, give a coherent picture of the changes of conformation of PEG and PEI in organic acid solvents. We find that PEG molecules, which form helices in isobutyric acid, also form helices in propanoic acid and isopentanoic acid. We show that PEI, which differs from PEG in the substitution of −NH− for −O− in the polymer backbone, also forms helices in isobutyric acid. While we previously observed a coexistence of coils and helices for PEG at molecular masses of 20 kg/mol and greater in isobutyric acid,[24] we observe only helices for PEI (25 kg/mol) in isobutyric acid. We find that PEI molecules remain helical to higher temperatures than do their PEG analogues. We confirm that PEI, like PEG, forms coils in D_2O and in H_2O.

Our hypothesis as to why PEG and PEI form helices in carboxylic acids is that the trace water present in the hygroscopic polymers when the solutions are prepared forms a hydration layer that stabilizes the polymer helices. The polymer helices fold and unfold as the trace water is added or removed.

Water is known to play an essential role in structure, stability, and dynamics of biopolymers. Levy and co-workers[45] have reported the importance of solvent effects on the helix conformation, in particular the folding kinetics of polyalanine. Mukherjee and co-workers[46] showed that peptides in water have coil conformations but fold into helices when reverse micelles are used to remove most of the bulk water. Chatani et al. report that PEI helices in the crystal can unfold into a planar zigzag conformation when the crystal becomes hydrated—just the opposite our observation of folding into a helices upon hydration in solution.[19]

Our studies to date have revealed three ways in which the polymers PEG and PEI, dissolved in carboxylic acids with carbon chain lengths of 3, 4, or 5, undergo helix-to-coil transitions. First, in the "pure" (but not anhydrous) solvents, helices form near room temperature and gradually unfold into coils as the temperature is increased, reaching complete unfolding at a transition temperature. Second, in the pure (but not anhydrous) solvents, helices form when trace water is present and unfold when the trace water is removed. Third, helices in a solution of isobutyric acid + water at the critical solution composition form coils at temperatures well above the critical solution temperature, form helices as the temperature is lowered, and unfold again into coils when very near the critical temperature.[25]

There are thus two thermally induced helix-to-coil transitions for these polymers: one that occurs on heating in pure organic acid solvents and their aqueous mixtures, and one that occurs on cooling near the liquid−liquid critical point (of isobutyric acid and water). Transitions that occur on heating require that the entropy change and the enthalpy change for the transition be positive and are thus entropically driven. In the case of PEG and PEI in organic acids, this increase in entropy can be related to a release of the water of hydration. Transitions that occur on cooling require that the entropy change and the enthalpy change for the transition be negative and are thus enthalpically driven. The uncoiling of the polymer helices near the critical point may be related to the dissolution of the polymer in the large water-rich fluctuations.[25]

We understand now that the presence of water is critical to the polymer conformations in these organic solvents. We do not understand the detailed role of the water, and we do not understand why this phenomenon occurs only in particular solvents.

Acknowledgment. This research was supported by the National Science Foundation, Chemistry Division. We also acknowledge support of the National Institute of Standards and Technology (NIST), Department of Commerce, in providing the neutron research facilities used in this work. Certain products and equipment are mentioned by name only to clarify the

experimental conditions used; this does not mean that they are the best for the purpose or that NIST endorses them. We are grateful to Susan Gregurick and Hailiang Zhang at the University of Maryland Baltimore County for their advice with the LORES software. We thank Sasha E. Knowlton for help with the polarimetry and Boualem Hammouda and Bryan Greenwald for their kind assistance with the SANS instrument.

Supporting Information Available: More graphs of the polarimetry data and more information on the choice of chiral dopants. This material is available free of charge via the Internet at http://pubs.acs.org.

References and Notes

(1) Yu, K.; Eisenberg, A. *Macromolecules* **1996**, *32*, 6359−6361.
(2) Dereci, L.; Ledger, S.; Mai, S.; Booth, C.; Hamley, I. W.; Pedersen, J. S. *Phys. Chem. Chem. Phys.* **1999**, *1*, 2773−2785.
(3) Li, H.; Yu, G.-E.; Price, C.; Booth, C.; Fairclough, J. P. A.; Ryan, A. J.; Mortensen, K. *Langmuir* **2003**, *19*, 1075−1081.
(4) Norman, A. I.; Fairclough, J. P. A.; Mai, S.; Ryan, A. J. *J. Macromol. Sci., Part B: Phys.* **2004**, *43*, 71−94.
(5) Norman, A. I.; Ho, D. L.; Lee, J.-H.; Karim, A. *J. Phys. Chem. B* **2006**, *110*, 62−67.
(6) Luo, L.; Eisenberg, A. *Langmuir* **2001**, *17*, 6804−6811.
(7) Lasic, D. D. *Vesicles*; Marcel Dekker: New York, 1996.
(8) Allen, C.; Maysinger, D.; Eisenberg, A. *Colloids Surf., B* **1999**, *16*, 3−27.
(9) Ding, J.; Liu, G. *J. Phys. Chem. B* **1998**, *102*, 6107−6113.
(10) Takahashi, Y.; Tadokoro, H. *Macromolecules* **1973**, *6*, 672−675.
(11) Yang, R.; Yang, X. R.; Evans, D. F.; Hendrikson, W. A.; Baker, J. *J. Phys. Chem.* **1990**, *94*, 6123−6125.
(12) Bailey, F. E.; Koleske, J. V. *Alkylene Oxides and Their Polymers*; Marcel Dekker: New York, 1991; Vol. 35.
(13) Harris, J. M.; Zalipsky, S., Eds. *Poly(ethylene glycol): Chemistry and Biological Applications*; American Chemical Society: Washington, DC, 1997; Vol. 680.
(14) http://www.shokubai.co.jp/productlist_pdf/product_e2_none.pdf.
(15) Abdallah, B.; Hassan, A.; Benoist, C.; Goula, D.; Behr, J. *Hum. Genet. Ther.* **1997**, *7*, 1947−1954.
(16) Remy, J. S.; Abdallah, B.; Zanta, M. A.; Boussif, O.; Behr, J. P.; Demeneix, B. *Adv. Drug Delivery Rev.* **1998**, *30*, 85−95.
(17) Fischer, D.; Bieber, T.; Li, Y. X.; Elsasser, H. P.; Kissel, T. *Pharm. Res.* **1999**, *16*, 1273−1279.
(18) Chantani, Y.; Kobatake, T.; Tadokoro, H.; Tanaka, R. *Macromolecules* **1982**, *15*, 170−176.
(19) Chantani, Y.; Tadokoro, H.; Saegusa, T.; Ikeda, H. *Macromolecules* **1981**, *14*, 315−321.
(20) Chantani, Y.; Kobatake, T.; Tadokoro, H. *Macromolecules* **1983**, *16*, 199−204.
(21) Greer, S. C. *Phys. Rev. A* **1976**, *14*, 1770−1780.
(22) Venkataraman, T. S.; Narducci, L. M. *J. Phys. C: Solid State Phys.* **1977**, *10*, 2849−2861.
(23) Shresh, R. S.; MacDonald, R. C.; Greer, S. C. *J. Chem. Phys.* **2002**, *117*, 9037−9049.
(24) Alessi, M. L.; Norman, A. I.; Knowlton, S. E.; Ho, D. L.; Greer, S. C. *Macromolecules* **2005**, *38*, 9333−9340.
(25) Castellanos, P.; Norman, A. I.; Greer, S. C. *J. Phys. Chem. B* **2006**, *110*, 22172−22177.
(26) Vennaman, N.; Lechner, M. D.; Oberthuer, R. C. *Polymer* **1987**, *28*, 1738−1748.
(27) Glinka, C. J.; Barker, J. G.; Hammouda, B.; Krueger, S.; Moyer, J. J.; Orts, W. J. *J. Appl. Crystallogr.* **1998**, *34*, 430−445.
(28) Weyerich, B.; Brunner-Popela, J.; Glatter, O. *J. Appl. Crystallogr.* **1999**, *32*, 197−209.
(29) Zhou, J.; Deyhim, A.; Krueger, S.; Gregurick, S. K. *Comput. Phys. Commun.* **2005**, *170*, 186−204.
(30) Higgins, J. S.; Benoit, H. C. *Polymers and Neutron Scattering*; Clarendon Press: Oxford, 1994.
(31) Porod, G. *Kolloid Z.* **1951**, *124*, 83−114.
(32) http://www.ncnr.nist.gov/resources/sansmodels.
(33) Pedersen, J. S. In *Neutrons, X-rays, and Light Scattering Methods Applied to Soft Condensed Matter*; Lindner, P., Zemb, T., Eds.; Elsevier Science B.V.: Amsterdam, 2002; p 400.
(34) Pedersen, J. S.; Schurtenberger, P. *Macromolecules* **1996**, *29*, 7602−7612.
(35) Glatter, O. In *Neutrons, X-rays, and Light: Scattering Methods Applied to Soft Condensed Matter*; Lindner, P., Zemb, T., Eds.; Elsevier: Amsterdam, 2002; p 103.
(36) GIFT software available from O. Glatter, University of Graz, Austria. Details can be found at the Web site http://physchem.kfunigraz.ac.at/sm/.
(37) Glatter, O. *J. Appl. Crystallogr.* **1977**, *10*, 415−421.
(38) Glatter, O. *J. Appl. Crystallogr.* **1980**, *13*, 577−584.
(39) Hansen, S. *J. Appl. Crystallogr.* **2003**, *36*, 1190−1196.
(40) Green, M. M.; Park, J.-W.; Sato, T.; Teramoto, A.; Lifson, S.; Selinger, R. L. B.; Selinger, J. V. *Angew. Chem., Int. Ed.* **1999**, *38*, 3138−3154.
(41) Nozaki, Y.; Tanford, C. *J. Biol. Chem.* **1963**, *238*, 4074−4082.
(42) Engdahl, A.; Nelander, B. *J. Chem. Phys.* **1987**, *86*, 1819−1823.
(43) Norman, A. I.; Ho, D. L.; Karim, A.; Amis, E. J. *J. Colloid Interface Sci.* **2005**, *288*, 155−165.
(44) Glatter, O. In *Neutron, X-ray, and Light Scattering: Introduction to an Investigative Tool for Colloidal and Polymeric Systems*; Lindner, P., Zemb, T., Eds.; North-Holland: New York, 1991; pp 33−82.
(45) Levy, Y.; Jortner, J.; Becker, O. M. *Proc. Natl. Acad. Sci. U.S.A.* **2001**, *98*, 2188−2193.
(46) Mukherjee, S.; Chowdhury, P.; Gai, F. *J. Phys. Chem. B* **2006**, *110*, 11615−11619.

MA0622783